Symmetric Nearly Shift-Invariant Tight Frame Wavelets

A. Farras Abdelnour, *Member, IEEE,* and Ivan W. Selesnick, *Member, IEEE*

***Abstract*—K-regular two-band orthogonal filterbanks have been applied to image processing. Such filters can be extended into a case of downsampling by two and more than two filters provided that they satisfy a set of conditions. Such a setup allows for more degrees of freedom but also at the cost of higher redundancy. The latter depends directly on the number of the wavelet filters involved. Tight frame filters allow the design of smooth scaling functions and wavelets with a limited number of coefficients. Moreover, such filters are nearly shift invariant, a desirable feature in many applications. In this paper, we explore a family of symmetric tight frame finite impulse response (FIR) filters characterized by the relations $H_3(z) = H_0(-z)$ and $H_2(z) = H_1(-z)$. They are simple to design and exhibit a degree of near orthogonality, in addition to near shift invariance. Both properties are desirable for noise removal purposes.**

***Index Terms*—Denoising, frame, symmetric filterbanks, wavelet transform.**

I. Introduction

As is well known, two-band finite impulse response (FIR) orthogonal filterbanks do not allow for symmetry except for the Haar filterbank. In addition, imposing orthogonality for the two-band FIR case requires relatively long filter support for such properties as high smoothness of resulting scaling function and wavelets and high approximation order. It is possible to obtain both symmetry and orthogonality for the case of more than two bands filterbanks (see, for example, [16], [19], and [27]), but smooth scaling and wavelet functions still require relatively long filters. For example, a Daubechies lowpass filter of length 8 possesses four zeros at $z = -1$ but lacks symmetry, while a tight frame lowpass filter of similar length allows for five zeros at $z = -1$, symmetry, and a visibly improved smoothness. In addition, due to the critical sampling, orthogonal filters suffer a pronounced lack of shift invariance.

The desirable properties can be achieved through the design of tight frame filterbanks, of which orthogonal filters are a special case. The redundancy of tight frame filters is such that it allows for an approximate shift invariance behavior due to the dense time-scale plane when compared with the case of orthogonal filters. In particular, the issue of shift invariance has been addressed by Kingsbury in [17] and [18], where complex wavelets with real and imaginary parts approximating Hilbert pairs are proposed for noise removal. In addition to symmetry, the proposed filterbanks are shorter and result in smoother scaling and wavelet functions. The theory of tight frame is by now well documented [4], [9], [10], [23]. In addition, two-dimensional (2-D) dual wavelets tight frames are discussed in [15]. Tight frame filterbanks (oversampled filterbanks) have seen use in noise removal applications (see, for example, [3], [8], [22], and [26]). The issue of tight frame wavelet design has been undertaken by a number of papers (see, in particular, [5], [21], and [25]). In more recent papers, Daubechies *et al.* [11] discuss filterbanks based on spline and pseudo-spline tight frames. In [6], Chui *et al.* address the design of shift-invariant wavelets obtained after relaxing tight frame condition.

In this paper, we discuss the design of a bank of four tight frame symmetric filters $\{h_0, h_1, h_2, h_3\}$ taking on the form $H_3(z) = H_0(-z)$ and $H_2(z) = H_1(-z)$ using Gröbner method [2], [7] and software Singular [14]. Additionally, it turns out that such filters can be designed using spectral factorization, as has been done in [5]. Examples using both methods and representing new wavelets will be discussed.

The paper is organized as follows: In Section II, the tight frame theory is briefly discussed. Issues such as lowpass filter minimum length and filterbank redundancy, among others, are addressed. In Section III, the family of tight frame filters of the form $H_3(z) = H_0(-z)$ and $H_2(z) = H_1(-z)$ is discussed. It is shown that they can be fully described through the polyphase components $H_{00}(z)$ and $H_{10}(z)$. Furthermore, given the (symmetric even length) lowpass filter $H_0(z)$, it is shown that the filters can be constructed starting with the polyphase component $H_{00}(z)$. Section IV describes design algorithm based on spectral factorization, which generates a filterbank of four tight frame symmetric even length filters. In Section V, different filterbanks are discussed as design examples. We address filterbank design for Gröbner method as well as spectral factorization. In addition, an example depicts an application of tight frame symmetric wavelets designed in this paper to noise removal. Section VI compares the Gröbner method, with spectral factorization with the advantages and drawbacks of both approaches, then concludes the paper.

II. Properties and Conditions

The theory of filterbanks and frames has been discussed and analyzed (see, for example, [4], [9], and [10]). Here, we introduce the basic concepts of frame theory. A set of wavelets

Manuscript received January 23, 2003; revised November 4, 2003. This material is based on work supported by the National Science Foundation under Grant 9875452. The associate editor coordinating the review of this manuscript and approving it for publication was Dr. Ta-Hsin Li.

A. F. Abdelnour is with Medical Physics, Memorial Sloan–Kettering Cancer Center, New York, NY 10021 USA (e-mail: abdelnoa@mskcc.org).

I. W. Selesnick is with the Department of Electrical and Computer Engineering, Polytechnic University, Brooklyn, NY 11201 USA (e-mail: selesi@poly.edu).

Digital Object Identifier 10.1109/TSP.2004.838959

$\psi_i, i = 1 \dots N-1$ constitutes a frame when for $0 < A \leq B < \infty$ and any function $f \in L^2$, we have [10], [15]

$$A\|f\|^2 \leq \sum_{i=1}^{N-1} \sum_{m,n} |\langle f, \psi_i(2^m \cdot -n)\rangle|^2 \leq B\|f\|^2$$

where A and B are known as frame bounds. The special case of $A = B$ is known as *tight frame*, and we obtain the following spaces:

$$\mathcal{V}_j = \operatorname*{Span}_n\{\phi(2^j t - n)\}$$
$$\mathcal{W}_{i,j} = \operatorname*{Span}_n\{\psi_i(2^j t - n)\}, \quad i = 1 \dots N-1$$

with

$$\mathcal{V}_j = \mathcal{V}_{j-1} \cup \mathcal{W}_{1,j-1} \cup \mathcal{W}_{2,j-1} \cup \cdots \cup \mathcal{W}_{N-1,j-1}$$

and the corresponding scaling function and wavelets satisfy the following multiresolution equations:

$$\phi(t) = \sqrt{2}\sum_n h_0(n)\phi(2t-n)$$
$$\psi_i(t) = \sqrt{2}\sum_n h_i(n)\phi(2t-n), \quad i = 1 \dots N-1.$$

Now, the bounds A and B take on the value [4]

$$A = B = \frac{1}{2}\sum_{i=0}^{N-1} \|h_i\|^2.$$

A. Oversampled Filterbanks

The frame condition can be expressed in terms of oversampled polyphase filters [30]. Given a set of N filters, we define them in terms of their polyphase components:

$$H_i(z) = H_{i,0}(z^2) + z^{-1}H_{i,1}(z^2), \quad i = 0 \dots N-1$$

where

$$H_{ij}(z) = \sum_n h_i(2n-j)z^{-n}, \quad j = 0, 1.$$

Now define the polyphase analysis matrix as

$$\mathbf{H}(z) = \begin{pmatrix} H_{0,0}(z) & H_{0,1}(z) \\ H_{1,0}(z) & H_{1,1}(z) \\ \vdots & \vdots \\ H_{N-1,0}(z) & H_{N-1,1}(z) \end{pmatrix}.$$

Now, if we define a signal $X(z)$ in terms of its polyphase components, then we have

$$\mathbf{x}(z) = (\, X_0(z) \quad X_1(z)\,)^T$$

where $X_j(z), j = 0, 1$ is defined in terms of the time domain signal $x(n)$ as follows:

$$X_j(z) = \sum_n x(2n-j)z^{-n}.$$

Then, the overall output signal $\hat{X}(z)$ of the analysis/synthesis filterbank can be expressed as

$$\hat{X}(z) = (\, 1 \quad z^{-1}\,)\,\mathbf{H}^T(z^2)\mathbf{H}(z^{-2})\mathbf{x}(z^2)$$

and to meet perfect reconstruction condition $\hat{X}(z) = X(z)$, we require that

$$\mathbf{H}^T(z)\mathbf{H}(z^{-1}) = \mathbf{I}$$

or we obtain

$$\sum_k H_{k,i}(z)H_{k,j}(z^{-1}) = \begin{cases} 1, & \text{if } i = j = 0 \\ 0, & \text{otherwise.} \end{cases}$$

Alternately, [24] shows that a three-band tight frame filterbank PR conditions can be expressed in terms of the Z-transforms of the filters $\{h_0, h_1, h_2\}$. It is easy to extend the PR conditions to N filters downsampled by 2:

$$\sum_{n=0}^{N-1} H_n(z)H_n(z^{-1}) = 2 \tag{1}$$
$$\sum_{n=0}^{N-1} H_n(-z)H_n(z^{-1}) = 0. \tag{2}$$

Last, it is shown in [5] and [20] that a necessary condition for the filterbank to exist is to have the filters $H_i(z), i = 0 \dots N-1$ each satisfy the following inequality:

$$|H_i(z)|^2 + |H_i(-z)|^2 < 2, \quad |z| = 1. \tag{3}$$

Notice that equality reduces to the traditional case of two-band orthogonal filterbank.

B. Constraints on the Length of h_0

It is shown in [24] that a three-band tight frame with downsampling by 2 and satisfying PR the minimum length of the lowpass filter h_0 is subject to the condition

$$\text{length } h_0 \geq K_0 + \min(K_1, K_2) \tag{4}$$

where K_0 is the number of zeros at $z = -1$ for the filter $H_0(z)$, and K_i is the number of zeros at $z = 1$ for the filters $H_i(z), i = 1, 2$. It is straightforward to extend condition (4) to the case of N filters. In that case, we obtain for h_0's minimum length

$$\text{length } h_0 \geq K_0 + \min(K_1, K_2, \dots, K_{N-1}). \tag{5}$$

Now, given the lower bound (5) on length h_0, the additional property of symmetry implies tighter constraint on the minimum length. Indeed, assuming a symmetric tight frame lowpass filter $H_0(z) = (1 + z^{-1})^{K_0}Q_0(z)$ of even length N_0 and with K_0 odd, we require that the factor $Q_0(z)$ of odd length $N_0 - K_0$ be symmetric, or we require $(N_0 - K_0 - 1)/2$ equations for symmetry. Then, the minimum length of h_0 now takes on the form

$$N_0 \geq K_0 + \min(K_1, K_2, \dots, K_{N-1}) + \frac{N_0 - K_0 - 1}{2}$$

and we obtain the minimum length of a symmetric h_0 as follows:

$$\text{length } h_0 \geq K_0 + 2\min(K_1, K_2, \ldots, K_{N-1}) - 1 \quad (6)$$

or in terms of $Q_0(z)$, we obtain

$$\text{length } q_0 \geq 2\min(K_1, K_2, \ldots, K_{N-1}) - 1.$$

Clearly, the length of q_0 is partly determined by the lowpass filter's symmetry and the wavelets' zero moments. In particular, in the four-band case with $K_3 = K_0, K_2 = K_1 + 1$, the inequality (6) becomes

$$\text{length } h_0 \geq K_0 + 2K_1 - 1$$

with equality achieved in case of minimum length filters.

C. Near Orthogonality

The near orthogonality of the spaces spanned by the resulting tight frame filters and their shifts is observed. It will be seen that there is an extent of near orthogonality to the filters' even shifts with respect to themselves as well as to other filters. This in turn reflects the degree of orthogonality in the scaling and wavelets functions $\{\phi, \psi_1, \psi_2, \psi_3\}$ and their integer shifts. We will use $\theta(h_i, h_j, m)$ to indicate the angle between two vectors h_i and h_j shifted with respect to each other by m, defined as

$$\theta(h_i, h_j, m) = \arccos\left(\frac{\langle h_i(n), h_j(n-m)\rangle}{\|h_i\| \cdot \|h_j\|}\right).$$

D. Near Shift Invariance

As is well known, wavelet systems are in general not shift invariant. However, such behavior can be approximated using redundant sets of filters. Following Kingsbury [17], [18] to evaluate the extent of shift invariance at the ith stage, a discrete unit step function $u(n - n_0), 0 \leq n_0 \leq 2^d - 1$ is fed into an iterated filterbank, with d being the number of stages. Then, the consistency of the output due only to the lowpass filter at the dth stage over all possible 2^d shifts is observed. A similar procedure is followed with the wavelet filters. Here, we consider the output due to all three wavelet filters at the dth stage. It is desired that the resulting outputs be as similar as possible for all shifts. It will be shown that there is an extent of shift invariance in the filters discussed in this paper.

E. Redundancy

A tight frame analysis system generates more data at the output than at the input. The redundancy rate depends on the number of filters N as well as the number of filtering stages d. For a single-stage filterbank, the redundancy ratio is $R = (N/2)$. For multiple stages, we have the contribution due to the lowpass filter and its following stages in addition to the highpass/bandpass filters. As such, the redundancy ratio at the ith stage is $(N-1)/2^i$ in addition to the lowpass filter contribution $1/2^i$. At the analysis output, the latter is just $1/2^d$. Putting the above results together, we have

$$R = (N-1)\left(\frac{1}{2} + \frac{1}{2^2} + \cdots + \frac{1}{2^{d-1}}\right) + \frac{N}{2^d}$$
$$= (N-1)\left(1 - \frac{1}{2^{d-1}}\right) + \frac{N}{2^d}. \quad (7)$$

From (7), we have $R \to N-1$ as $d \to \infty$ and $R = (N/2)$ for $d = 1$. It is clear that for a fixed N, (7) has monotonous behavior. In general, the redundancy R is bounded by $(N/2) \leq R \leq N-1$. For the case of $N = 4$, we have $R = 3$ for $d \to \infty$, while $d = 4$ results in $R = 23/8 \approx 3$.

F. Smoothness versus K_0

One of the advantages of tight frame filterbanks is the possibility of achieving high K_0 with an accompanying high degree of smoothness ν_2 without a necessarily large support of h_0, as will be seen shortly. We note that the orthogonal case, on the other hand, has typically low smoothness for a given K_0. It is shown in [28] that the highest possible derivative ν_2 for a scaling function $\phi(\cdot)$ given the corresponding $h_0(n)$ is bounded by $\nu_2 < K_0$. Smoothness is measured using the Sobolev exponent of a scaling function ϕ, which is defined as [13], [31]

$$\nu_2(\phi) := \sup\left\{\nu_2 : \int_{-\infty}^{\infty} |\Phi(\omega)|^2 (1 + |\omega|^2)^{\nu_2}\, d\omega < \infty\right\}.$$

The actual computation of ν_2 is found using [16], and for the normalization $\sum_n h_0(n) = \sqrt{2}$, we have

$$\nu_2 = -\frac{1}{2}\log_2 \lambda_{\max}$$

where $\lambda_{\max}$ is the largest eigenvalue of a matrix generated by $(c_{2i-j})_{-N \leq i,j \leq N}$ with $c(z) = Q_0(z)Q_0(z^{-1})$ and $Q_0(z)$ known from $H_0(z) = (1 + z^{-1})^{K_0} Q_0(z)$.

III. Case $H_3(z) = H_0(-z), H_2(z) = H_1(-z)$

We now consider the particular case of a tight frame symmetric wavelet system consisting of two filters and their modulated versions. Such a system reduces the required degrees of freedom, and in general, each filter covers distinct frequency band. The resulting wavelets vary in the rate of oscillation, allowing one to capture various features of a signal. In addition, the accuracy K_0 directly determines the number of moments K_3 of $h_3(n)$, with $K_3 = K_0$. Two design methods are offered: One method relies on Gröbner basis, proposed in [2] and [7] and can be used to design the filters, as depicted in Example 1. In the second method, we propose an alternative method based on spectral factorization and exploiting the polyphase structure of the filterbank to generate the filters starting with $H_{00}(z)$. It is important to note that in the following derivation, we assume that the filters are of even length; thus, K_0 is necessarily odd. Two filters are symmetric, and two are antisymmetric. Now, from $H_3(z) = H_{30}(z^2) + z^{-1}H_{31}(z^2)$ and $H_3(z) = H_0(-z)$, we have

$$H_3(z) = H_{00}(z^2) - z^{-1}H_{01}(z^2).$$

Similarly, for $H_2(z)$, we have

$$H_2(z) = H_{10}(z^2) - z^{-1}H_{11}(z^2).$$

On the unit circle, we have $H_3(e^{j\omega}) = H_0(e^{j(\omega+\pi)})$ and $H_2(e^{j\omega}) = H_1(e^{j(\omega+\pi)})$, but from (1), the following condition needs to be satisfied, with $z = e^{j\omega}$:

$$|H_0(e^{j\omega})|^2 + |H_1(e^{j\omega})|^2 + |H_2(e^{j\omega})|^2 + |H_3(e^{j\omega})|^2 = 2$$

which gives [32]

$$|H_1(e^{j\omega})|^2 + \left|H_1(e^{j(\omega+\pi)})\right|^2 = 2 - |H_0(e^{j\omega})|^2 - \left|H_0(e^{j(\omega+\pi)})\right|^2.$$

In the time domain, we have

$$r_0(n) + r_1(n) + r_2(n) + r_3(n) = 2\delta(n)$$

where $r_i(n)$ is the autocorrelation of h_i, defined as $r_i(n) = \sum_k h_i(k)h_i(k-n)$, or we have

$$(1 + (-1)^n)(r_0(n) + r_1(n)) = 2\delta(n)$$

which reduces to

$$r_0(2n) + r_1(2n) = \delta(n). \tag{8}$$

The above equation suggests a dependence of the filter h_1 (and, thus, h_2) on h_0. Evaluating (8) at $n = 0$, and from $r_2(n) = (-1)^n r_1(n)$, we obtain

$$r_0(0) + r_1(0) = 1.$$

We also note that such a structure immediately implies that h_3 and h_0 are orthogonal to all their even shifts, and so are h_2 and h_1 or

$$\sum_n h_0(n)h_3(n-2k) = 0 \quad \forall k \in \mathbb{Z}.$$

This can be shown as follows:

$$\sum_n h_0(n)h_3(n-2k) = \sum_n h_0(n)h_0(n-2k)(-1)^{n-2k}$$

or, with $h_{01}(m) = h_{00}(l_0 - 1 - m)$, we have

$$\begin{aligned}\sum_n &(-1)^n h_0(n)h_0(n-2k)\\ &= \sum_m h_0(2m)h_0(2m-2k)\\ &\quad - \sum_m h_0(2m+1)h_0(2m+1-2k)\\ &= \sum_m h_{00}(m)h_{00}(m-k)\\ &\quad - h_{00}(l_0-1-m)h_{00}(l_0-1-m+k) = 0\end{aligned}$$

where l_0 is given by $l_0 = \text{length} h_{00}$. Orthogonality of h_1 and h_2 can be proved similarly.

In the following, we state two main results of the paper [(9) and (10)] with the proofs in the accompanying Appendix. All filters are symmetric/antisymmetric and are of even length.

$$\begin{aligned}H_0(z) &= H_{00}(z^2) + z^{-(2l_0-1)}H_{00}(z^{-2})\\ H_1(z) &= H_{10}(z^2) + z^{-(2l_0-1)}H_{10}(z^{-2})\\ H_2(z) &= H_{10}(z^2) - z^{-(2l_0-1)}H_{10}(z^{-2})\\ H_3(z) &= H_{00}(z^2) - z^{-(2l_0-1)}H_{00}(z^{-2})\end{aligned} \tag{9}$$

and

$$H_{10}(z)H_{10}(z^{-1}) = \frac{1}{2} - H_{00}(z)H_{00}(z^{-1}). \tag{10}$$

Clearly, the filters in (9) are now expressed only in terms of $H_{00}(z)$ and $H_{10}(z)$.

It turns out that given the filters $H_3(z) = H_0(-z)$, the structure of $H_2(z)$ is such that both $H_2(z) = H_{20}(z^2) + z^{-1}H_{21}(z^2)$ and $H_2(z) = H_{21}(z^2) + z^{-1}H_{20}(z^2)$ satisfy the TF conditions. Thus, given a tight frame lowpass symmetric filter $H_0(z)$, there exists an even number of filter sets $\{h_1, h_2, h_3\}$ that satisfy PR, with $H_2(z) = H_1(-z)$ and $H_3(z) = H_0(-z)$. To show this, we consider the filter $H_2(z)$, which is now defined as follows:

$$H_2(z) = -z^{-2(l_0-1)}H_{10}(z^{-2}) + z^{-1}H_{10}(z^2).$$

Then, with $H_1(z) = H_2(-z)$, the polyphase matrix becomes the equation shown at the bottom of the page, with $\alpha = z^{-(l_0-1)}$, and l_0 defined as $l_0 = \text{length} h_{00}$, as above. Then, to satisfy perfect reconstruction condition, we require that

$$\mathbf{H}^T(z)\mathbf{H}(z^{-1}) = \mathbf{I}.$$

$$\mathbf{H}^T(z) = \begin{pmatrix} H_{00}(z) & \alpha H_{10}(z^{-1}) & -\alpha H_{10}(z^{-1}) & H_{00}(z) \\ \alpha H_{00}(z^{-1}) & H_{10}(z) & H_{10}(z) & -\alpha H_{00}(z^{-1}) \end{pmatrix}$$

Multiplying out and evaluating the elements of $\mathbf{H}^T(z)\mathbf{H}(z^{-1})$, we have

$$H_{00}(z)H_{00}(z^{-1}) + H_{10}(z)H_{10}(z^{-1}) = \frac{1}{2}.$$

Thus, if $H_2(z) = H_{20}(z^2) + z^{-1}H_{21}(z^2)$ is a solution satisfying tight frame and symmetry conditions, then so is $H_2(z) = H_{21}(z^2) + z^{-1}H_{20}(z^2)$, with $H_2(z) = H_1(-z)$.

IV. Spectral Factorization Method

Equations (9) and (10) suggest that the entire system can be found once $H_0(z)$, and thus, $H_{00}(z)$ is given. To generate the tight frame filterbanks, we use the prototype filter defined in (11) and (12). By seeking tight frame symmetric filterbank, K_0 is no longer restricted to $K_0 < (1/2)$length h_0, as is the case with two-channel orthogonal filters. In fact, now, the only constraint is the minimal value chosen for K_2 or K_1, defining in turn the minimal length of h_0. One possible lowpass filter that generates the tight frame filterbank is given as follows:

$$H_0(z) = \left(\frac{1+z^{-1}}{2}\right)\left(\frac{1+2z^{-1}+z^{-2}}{4}\right)^r Q_0(z) \qquad (11)$$

where

$$Q_0(z) = \sum_{n=0}^{L} \binom{r+\frac{1}{2}+n-1}{n} \left(\frac{-1+2z^{-1}-z^{-2}}{4}\right)^n. \qquad (12)$$

$H_0(z)$ is of even length, and r is such that $K_0 = 2r+1$. With q_0 of length $2L+1$, the overall length of the filter h_0 is length $h_0 = 2(r+L+1)$. It is thus possible to start with (11) and obtain a family of tight frame symmetric filters by supplying the number of zeros $K_0 = 2r+1$ of h_0 at $z = -1$ as well as the length of q_0. In summary, given the parameters r and L, the design procedure goes as follows.

1) Choose the K_i's in terms of L and r as follows:

$$K_0 = 2r+1$$
$$K_1 = L+1+\frac{1}{2}(1+(-1)^L)$$
$$K_2 = L+2-\frac{1}{2}(1+(-1)^L)$$
$$K_3 = 2r+1.$$

2) Find $H_0(z)$ using (11) and (12).
3) Knowing $H_0(z)$ and, thus, $H_{00}(z)$, find $H_{10}(z)$ from (10) using spectral factorization.
4) Find $H_1(z)$ from $H_1(z) = H_{10}(z^2) + z^{-(2l_0-1)}H_{10}(z^{-2})$ with $l_0 = \text{length} h_{10}$.
5) Having found $H_{10}(z)$ from $H_{00}(z)$, the additional filters are obtained as follows: $H_2(z) = H_1(-z)$ and $H_3(z) = H_0(-z)$.

Remark: The above method is not only restricted to the lowpass filter described in (11) and (12) but can be used with any readily available tight frame even length lowpass filter taking on the form $H_0(z) = (1+z^{-1})^{K_0}Q_0(z)$ and satisfying inequality (3). Thus, given a lowpass tight frame filter h_0, it suffices to start the above filter design procedure at step 3.

V. Examples

Different sets of above discussed filterbanks are presented in this section. It will be shown that they are nearly shift invariant and approximate orthogonality in addition to the fact that they are all symmetric. In addition, due to the relation between the $\{h_0, h_1, h_2, h_3\}$ filters discussed in this paper, only the filters h_0 and h_1 are shown, the remaining wavelets being simply generated by modulated versions, given by $h_3(n) = (-1)^n h_0(n)$ and $h_2(n) = (-1)^n h_1(n)$. Example 1 illustrates Gröbner design filterbank, while Example 2 discusses wavelet design using spectral factorization method. For both examples, we tabulate the angles between the various filters and their even shifts with respect to each other. Example 3 illustrates an application of tight frame filterbanks to noise removal, with comparison with published filterbanks. Further design examples are discussed in [1].

A. Example I: Design Using Gröbner Methods

With $\{K_0, K_1, K_2, K_3\} = \{7, 2, 5, 7\}$, the associated Gröbner basis [2], [7] resulted in four distinct lowpass filters, with the parameter A in (14) taking on the values $A \in \{-0.007\,164, -0.006\,180, 0.000\,781, 0.030\,434\}$. The resulting filter $H_0(z)$ is given by

$$H_0(z) = \frac{1}{\sqrt{2}}(1+z^{-1})^7 Q_0(z) \qquad (13)$$

with

$$Q_0(z) = A(1+z^{-4}) - \left(4A - \frac{7}{512}\right) \times (z^{-1}+z^{-3}) + \left(6A - \frac{11}{256}\right)z^{-2}. \qquad (14)$$

Notice that this filter is distinct from the family defined in (11) and (12). For $A \approx 0.000\,781$, the resulting lowpass filter offers the highest smoothness coefficient with $\nu_2 \approx 5.1195$. This results in the filterbank listed in Table I (see also Table II). The filters corresponding to $\{K_0, K_1, K_2, K_3\} = \{7, 2, 5, 7\}$ are illustrated in Fig. 1. The resulting scaling function and wavelets are shown in Fig. 2. From Fig. 3, the filters exhibit a very nearly shift-invariant behavior.

B. Example 2: Design Using Spectral Factorization

To illustrate an example of spectral factorization design, we look for a set of filters satisfying $\{K_0, K_1, K_2, K_3\} = \{15, 4, 5, 15\}$, where K_0 is deliberately chosen high in order to depict the use of spectral factorization. Substituting in (11) and (12) with $r = 7$ and $L = 3$, we have

$$H_0(z) = \frac{\sqrt{2}}{2^{25}}(1+z^{-1})^{15}Q_0(z)$$

with

$$Q_0(z) = 49\,404z^{-3} - 1615(1+z^{-6}) + 11\,730(z^{-1}+z^{-5}) - 34\,305(z^{-2}+z^{-4}).$$

The scaling function and corresponding wavelets are shown in Fig. 4. Solving for $H_{10}(z)$ as described in Section IV, we obtain the filters depicted in Fig. 5. Table III lists the coefficients of the filters h_0 and h_1. For the sake of completeness, we mention the

TABLE I
EXAMPLE 1: FILTERBANK $\{h_0, h_1, h_2, h_3\}$ COEFFICIENTS FOR $K_0 = K_3 = 7, K_1 = 2$, AND $K_2 = 5$

n	$h_0(n)$	$h_1(n)$
0	-0.00055277114224	-0.00033767136406
1	-0.01132578895076	0.01854042113559
2	-0.03673606302189	-0.02613107863916
3	0.00608048256466	-0.21256591159938
4	0.23533603943029	-0.12220989795770
5	0.51430488230650	0.34270413842472
6	0.51430488230650	0.34270413842472
7	0.23533603943029	-0.12220989795770
8	0.00608048256466	-0.21256591159938
9	-0.03673606302189	-0.02613107863916
10	-0.01132578895076	0.01854042113559
11	-0.00055277114224	-0.00033767136406

TABLE II
EXAMPLE 1: ANGLES BETWEEN SPACES GENERATED BY FILTERS IN FIG. 1

shift	h_0,h_0	h_1, h_1	h_0,h_1	h_0,h_2	h_0,h_3
0	0	0	52.16	90	90
2	68.94	49.71	79.35	85.15	90
4	85.82	82.46	81.46	85.82	90
6	89.43	88.98	88.44	88.69	90
8	89.92	89.86	89.97	89.89	90
10	89.99	89.99	89.99	89.99	90

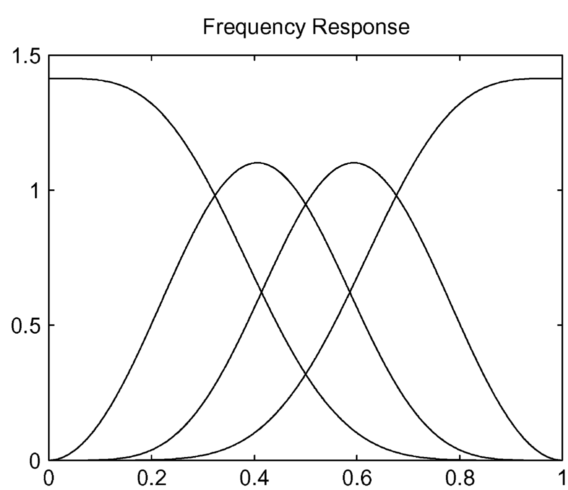

Fig. 1. Example 1: Gröbner designed filters with $\{K_0, K_1, K_2, K_3\} = \{7, 2, 5, 7\}$. Associated wavelets are illustrated in Fig. 2.

associated parameters. As to be expected, the scaling function is highly differentiable, with a degree of smoothness approximately $\nu_2 \approx 8.9194$. The extent of orthogonality between the filters and their various even shifts is depicted in Table IV. We can see that with the exception of $\theta(h_1, h_1, 2) = 40.68$, the filters and their shifts closely approximate orthogonality. Indeed, the angles between h_0 and h_2 and their even shifts are quite close to 90°. Additionally, the filters are very nearly shift invariant, as can readily be seen in Fig. 6.

C. Example 3: Applications

We consider in this section an example of applications of symmetric tight frame wavelets to the area of image processing and noise removal. We consider a symmetric filterbank, with $\{K_0, K_1, K_2, K_3\} = \{7, 2, 3, 7\}$ and a lowpass filter $H_0(z)$ of the form

$$H_0(z) = (1 + z^{-1})^7 (1 + z^{-1} + z^{-2}) Q_0(z). \qquad (15)$$

The filterbank can be obtained from http://taco.poly.edu/farras. This set of filters in particular has been chosen due to its favorable denoising performance. The filterbank's performance is compared with that of symmetric filterbanks with both two-channel biorthogonal filters and four-channel tight frame filterbanks. We will consider a 512×512 image subjected to additive

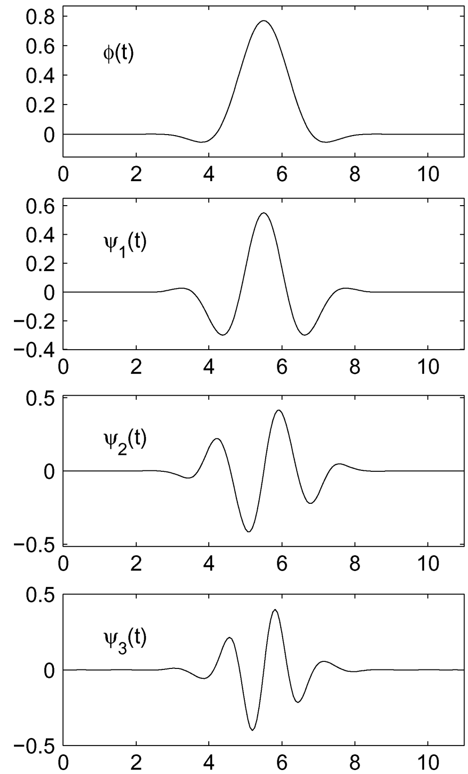

Fig. 2. Example 1: Wavelets corresponding to $\{K_0, K_1, K_2, K_3\} = \{7, 2, 5, 7\}$.

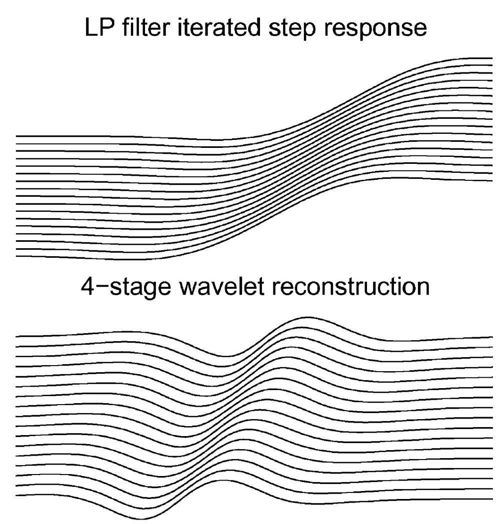

Fig. 3. Example 1: Near shift invariance corresponding to $\{K_0, K_1, K_2, K_3\} = \{7, 2, 5, 7\}$

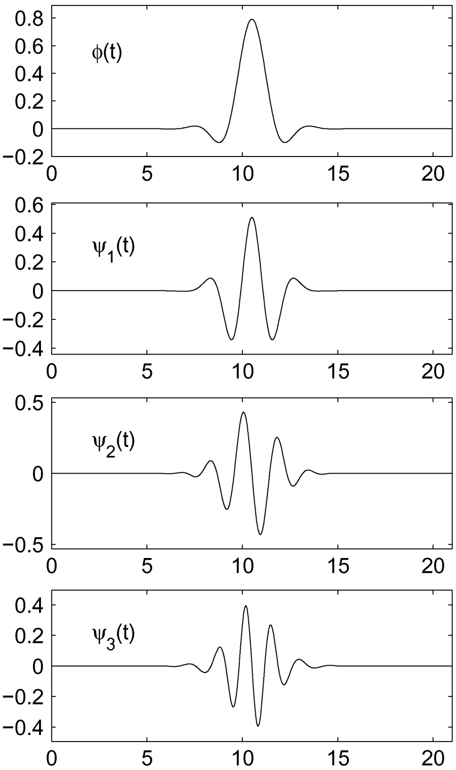

Fig. 4. Example 2: Wavelets and scaling function with $\{K_0, K_1, K_2, K_3\} = \{15, 4, 5, 15\}$.

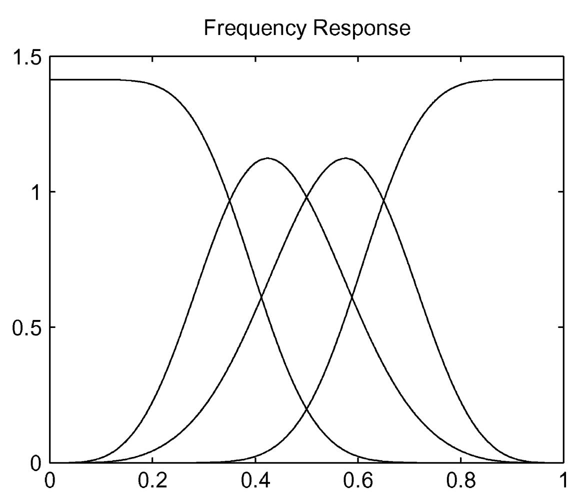

Fig. 5. Example 2: $\{K_0, K_1, K_2, K_3\} = \{15, 4, 5, 15\}$ filters designed through spectral factorization. Resulting wavelets are depicted in Fig. 4.

white Gaussian noise. Denoising is performed using the soft threshold, which is defined as

$$\hat{x} = \mathrm{sgn}(x)(|x| - \eta)_+$$

where η is some threshold. The measure of performance is peak signal to noise ratio, given by $\mathrm{PSNR} = 10\log_{10}((255^2/\mathrm{MSE}))$, with $\mathrm{MSE} = (1/M^2)\sum_{m,j}|x(m,j) - \hat{x}(m,j)|^2$, and where x is an $M \times M$ image, and $\hat{x}$ is the output. The threshold η is estimated from $\eta = \sqrt{2}\sigma_n$, where σ_n^2 is the noise variance estimate, which is found from the highpass outputs. More specifically,

TABLE III
BANDPASS FILTER h_1 COEFFICIENTS FOR EXAMPLE 2. $K_0 = K_3 = 15, K_1 = 4$, AND $K_2 = 5$

n	$h_0(n)$	$h_1(n)$
0	-0.00006806716035	0.00033470718376
1	-0.00052662487214	-0.00010709617646
2	-0.00117716147891	-0.00083815645134
3	0.00133411634276	-0.00184900827809
4	0.01000587257073	0.00040715239482
5	0.01000587257073	0.01797012314831
6	-0.02668232685528	0.05528765033433
7	-0.07024530947614	0.00398035279221
8	0.00400234902829	-0.21067061941896
9	0.26015268683895	-0.15449251248712
10	0.52030537367790	0.28997740695853
	⋮	⋮

TABLE IV
EXAMPLE 2: ANGLES BETWEEN SPACES GENERATED BY FILTERS IN FIG. 5

shift	h_0, h_0	h_1, h_1	h_0, h_1	h_0, h_2	h_0, h_3
0	0	0	62.12	90	90
2	69.93	40.68	77.99	83.77	90
4	82.18	72.50	83.60	84.51	90
6	89.40	88.68	84.02	88.03	90
8	89.25	88.35	88.91	89.63	90
10	89.73	89.41	89.96	89.95	90
12	89.97	89.95	89.92	89.98	90
14	89.99	89.99	89.98	89.99	90
16	89.99	89.99	89.99	89.99	90
18	89.99	89.99	89.99	89.99	90

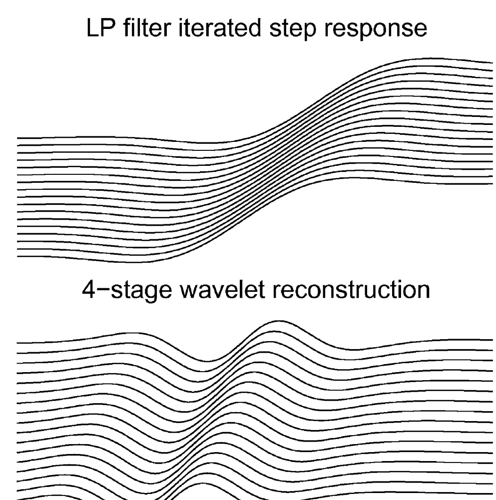

Fig. 6. Example 2: $\{K_0, K_1, K_2, K_3\} = \{15, 4, 5, 15\}$; near shift invariance.

the noise variance in the TF filterbank is estimated from the outputs of the first-stage filters $h_1(n_1)h_3(n_2), h_2(n_1)h_3(n_2)$, and $h_3(n_1)h_3(n_2)$. Notice the output of the filter resulting from $h_0(n_1)h_3(n_2)$ is not considered. In Table V, we compare the performances of various filterbanks with the tight frame symmetric filterbank with $H_0(z)$, as shown in (15). The filterbank is somewhat superior to the TF discussed in [5] as well as the symmetric biorthogonal filterbanks discussed in [10], [12], and [29]. Fig. 7 shows the result of soft thresholding when $\sigma_n = 0.075$. The noisy image pixels are normalized to [0, 1].

TABLE V
PSNR IN DECIBELS RESULTING FROM SOFT THRESHOLDING OF LENA IMAGE USING VARIOUS FILTERBANKS

σ_n	Proposed	TF [a]	7/9 [b]	9/15 [c]	6/10 [d]	10/18 [e]
0.05	79.8516	79.6792	79.4988	79.5886	79.6595	79.4445
0.075	77.7952	77.6056	77.4272	77.4680	77.4539	77.2934

[a] [5]
[b] [10, table 8.3]
[c] [10, table 8.5]
[d] [29, table 2]
[e] [12, table 3]

Fig. 7. Example 3: Noise removal for case $\sigma_n = 0.075$.

VI. CONCLUSION

The Gröbner basis method has proved its usefulness in filterbank design: It facilitates solving a system of nonlinear equations as is the case, for example, with orthogonal and tight frame filterbanks: It results in an exact solution within computer precision; it yields all solutions satisfying a set of constraints; and it is relatively easy to impose such constraints as symmetry or tight frame or filters of various lengths. For example, it was possible to find a tight frame symmetric filterbank given by $\{K_0, K_1, K_2, K_3\} = \{7, 2, 5, 7\}$ using Gröbner basis method. It is clear that Gröbner method allows one to generate a filterbank with a specific set of K_i's with the constraint of satisfying condition (6).

On the other hand, given a lowpass filter, the spectral factorization method makes it easy to find the filters $\{h_1, h_2, h_3\}$. Additionally, that results in all filterbanks satisfying the PR condition, which may or may not include more than one arrangement of the moments $\{K_1, K_2\}$, with the moments $K_0 = K_3$. For example, the lowpass filter resulting from Gröbner basis method described above can lead to bandpass filters with $\{K_1, K_2\} = \{2, 3\}$ in addition to $\{K_1, K_2\} = \{2, 5\}$. This allows one to obtain a larger pool of bandpass filters than those obtained using Gröbner basis method due to the fact that there are no restrictions beyond those imposed by the lowpass filter h_0.

Clearly, the Gröbner method allows one to design a filterbank *ex nihilo* with various properties, as depicted in Example 1. However, the method suffers the issues of required memory and time to find the associated Gröbner basis. On the other hand, spectral factorization is a simple method that nonetheless requires an available lowpass filter with the restrictions the latter imposes on the choices of $\{K_1, K_2\}$. It is clear that to each method, there are advantages and disadvantages.

We have presented a class of wavelets based on tight frame symmetric filterbanks that can be designed by using the Gröbner method or spectral factorization. In addition to their symmetry, the filters result in limit functions that are smoother than those resulting from orthogonal filters of comparable length. The dense time-frequency plane of tight frame filterbanks result in an approximate shift invariance. In addition, the filters discussed in this paper exhibit a degree of orthogonality. An example shows the advantage of using such filters for noise-removal purposes. Notice how the chosen threshold is global, that is, it is the same value for all stages. Clearly, the denoising performance can be improved by varying the threshold over the different stages. It would be interesting to exploit the redundancy of the oversampled filterbank and couple it with more sophisticated noise-removal algorithms.

APPENDIX

Exploiting symmetry, the filters $\{h_0, h_1, h_2, h_3\}$ can be described by only $H_{00}(z)$ and $H_{10}(z)$. By symmetry, we have $h_{01}(n) = h_{00}(l_0 - 1 - n)$ or

$$H_{01}(z) = \sum_n h_{00}(l_0 - 1 - n) z^{-n}$$

or with the substitution $l_0 - 1 - n = m$, we have

$$\sum_n h_{00}(l_0 - 1 - n) z^{-n} = z^{-(l_0-1)} \sum_m h_{00}(m) z^m$$

from which we get

$$H_{01}(z) = z^{-(l_0-1)} H_{00}(z^{-1}). \tag{A.1}$$

Similarly, for the case of $H_{11}(z)$, we have

$$H_{11}(z) = z^{-(l_0-1)} H_{10}(z^{-1}). \tag{A.2}$$

Now, the filters obeying the conditions $H_0(z) = H_3(-z)$ and $H_2(z) = H_1(-z)$ can be rewritten as follows:

$$\begin{aligned} H_0(z) &= H_{00}(z^2) + z^{-(2l_0-1)} H_{00}(z^{-2}) \\ H_1(z) &= H_{10}(z^2) + z^{-(2l_0-1)} H_{10}(z^{-2}) \\ H_2(z) &= H_{10}(z^2) - z^{-(2l_0-1)} H_{10}(z^{-2}) \\ H_3(z) &= H_{00}(z^2) - z^{-(2l_0-1)} H_{00}(z^{-2}). \end{aligned} \tag{A.3}$$

Then, to achieve perfect reconstruction, the following equation needs to be satisfied:

$$\mathbf{H}^T(z)\mathbf{H}(z^{-1}) = \mathbf{I} \tag{A.4}$$

where $\mathbf{H}^T(z)$ is given by

$$\mathbf{H}^T(z) = \begin{pmatrix} H_{00}(z) & H_{10}(z) & H_{20}(z) & H_{30}(z) \\ H_{01}(z) & H_{11}(z) & H_{21}(z) & H_{31}(z) \end{pmatrix}.$$

However, from (A.3), the above matrix can be written as the equation at the top of the next page, where A is a matrix accounting for the delay terms in (A.3) and is given by

$$A = \begin{pmatrix} 1 & 0 \\ 0 & z^{-(l_0-1)} \end{pmatrix}.$$

$$\mathbf{H}^T(z) = A \begin{pmatrix} H_{00}(z) & H_{10}(z) & H_{10}(z) & H_{00}(z) \\ H_{00}(z^{-1}) & H_{10}(z^{-1}) & -H_{10}(z^{-1}) & -H_{00}(z^{-1}) \end{pmatrix}$$

From (A.1) and (A.2), (A.3) and (A.4) reduce to the following equation relating $H_{00}(z)$ and $H_{10}(z)$ and, thus, $H_0(z)$ and $H_1(z)$:

$$H_{00}(z)H_{00}(z^{-1}) + H_{10}(z)H_{10}(z^{-1}) = \frac{1}{2}. \tag{A.5}$$

Equation (A.5) can be written slightly differently as follows:

$$H_{10}(z)H_{10}(z^{-1}) = \frac{1}{2} - H_{00}(z)H_{00}(z^{-1}). \tag{A.6}$$

References

[1] A. F. Abdelnour, "Wavelet Design Using Gröbner Basis Methods," Ph.D. dissertation, Polytechnic Univ., Brooklyn, NY, 2002.

[2] W. W. Adams and P. Loustaunau, *An Introduction to Gröbner Bases*. New York: American Math. Soc., 1994.

[3] H. Bölcskei and F. Hlawatsch, "Oversampled filter banks: Optimal noise shaping, design freedom, and noise analysis," in *Proc. IEEE Int. Conf. Acoust., Speech, Signal Process.*, vol. 3, 1997, pp. 2453–2456.

[4] H. Bölcskei, F. Hlawatsch, and H. G. Feichtinger, "Frame-theoretical analysis of oversampled filter banks," *IEEE Trans. Signal Process.*, vol. 46, no. 12, pp. 3256–3268, Dec. 1998.

[5] C. K. Chui and W. He, "Compactly supported tight frames associated with refinable functions," *Applied Comput. Harmonic Anal.*, vol. 8, pp. 293–319, 2000.

[6] C. K. Chui, W. He, and J. Stöckler, "Compactly supported tight and sibling frames with maximum vanishing moments," *Applied Comput. Harmonic Anal.*, vol. 13, pp. 224–262, Nov. 2002.

[7] D. Cox, J. Little, and D. O'Shea, *Ideals, Varieties, and Algorithms: An Introduction to Computational Algebraic Geometry and Commutative Algebra*. New York: Springer-Verlag, 1991.

[8] Z. Cvetković and M. Vetterli, "Overcomplete expansions and robustness," in *Proc. IEEE Int. Symp. Time-Frequency Time-Scale Analysis*, 1996, pp. 325–328.

[9] ——, "Oversampled filter banks," *IEEE Trans. Signal Processing*, vol. 46, no. 5, pp. 1245–1255, May 1998.

[10] I. Daubechies, *Ten Lectures on Wavelets*. Philadelphia, PA: SIAM, 1992.

[11] I. Daubechies, B. Han, A. Ron, and Z. Shen, Framelets: MRA-Based Constructions of Wavelet Frames, 2001. Preprint.

[12] F. M. de Saint-Martin, P. Siohan, and A. Cohen, "Biorthogonal filterbanks and energy preservation property in image compression," *IEEE Trans. Image Process.*, vol. 8, pp. 168–178, Feb. 1999.

[13] T. Eirola, "Sobolev characterization of solutions of dilation equations," *SIAM J. Math. Anal.*, vol. 23, pp. 1015–1031, July 1992.

[14] G.-M. Greuel, G. Pfister, and H. Schönemann. (1997, May) Reports on Computer Algebra. Cent. Comput. Algebra, Univ. Kaiserslautern, Kaiserslautern, Germany. [Online]. Available: http://www.singular.uni-kl.de/

[15] B. Han, "On dual wavelets tight frames," *Applied Comput. Harmonic Anal.*, no. 4, pp. 380–413, 1997.

[16] ——, "Symmetric orthonormal scaling functions and wavelets with dilation factor 4," *Adv. Comput. Math.*, no. 8, pp. 221–247, 1998.

[17] N. Kingsbury, "Shift invariant properties of the dual-tree complex wavelet transform," in *Proc. IEEE Int. Conf. Acoust., Speech, Signal Process.*, vol. 3, Mar. 15–19, 1999, pp. 1221–1224.

[18] ——, "A dual-tree complex wavelet transform with improved orthogonality and symmetry properties," in *Proc. IEEE Conf. Image Process.*, vol. 1429, Vancouver, BC, Canada, Sep. 11–13, 2000.

[19] S. Oraintara, T. D. Tran, P. N. Heller, and T. Q. Nguyen, "Lattice structure for regular paraunitary linear-phase filterbanks and M-band orthogonal symmetric wavelets," *IEEE Trans. Signal Process.*, vol. 49, no. 11, pp. 2659–2672, Nov. 2001.

[20] A. Petukhov, "Explicit construction of framelets," *Applied Comput. Harmonic Anal.*, vol. 11, pp. 313–327, Sep. 2001.

[21] ——, "Symmetric framelets," *Constructive Approx.*, vol. 19, no. 2, pp. 309–328, Jan. 2003.

[22] L. Rebollo-Neira, A. G. Constantinides, and T. Stathaki, "Signal representation for compression and noise reduction through frame-based wavelets," *IEEE Trans. Signal Process.*, vol. 46, no. 3, pp. 587–597, Mar. 1998.

[23] A. Ron and Z. Shen, "Construction of compactly supported affine frames in $L_2(\mathbb{R})$," *Electron. Prod.*, pp. 1–21, 1997.

[24] I. W. Selesnick, "Wavelets in signal and image analysis: From theory to practice," in *The Double Density Discrete Wavelet Transform*, A. Petrosian and F. G. Meyer, Eds. Boston, MA: Kluwer, 2001.

[25] ——, "Smooth wavelets tight frames with zero moments," *Applied Comput. Harmonic Anal.*, vol. 10, pp. 163–181, 2001.

[26] I. W. Selesnick and L. Şendur, "Smooth wavelet frames with application to denoising," in *Proc. IEEE Int. Conf. Acoust., Speech, Signal Process.*, vol. 1, June 5–9, 2000, pp. 129–132.

[27] A. K. Soman, P. P. Vaidyanathan, and T. Q. Nguyen, "Linear phase paraunitary filter banks: Theory, factorizations and designs," *IEEE Trans. Signal Process.*, vol. 41, no. 12, pp. 3480–3496, Dec. 1993.

[28] G. Strang and T. Nguyen, *Wavelets and Filter Banks*. Wellesley, MA: Wellesley-Cambridge, 1996.

[29] D. B. H. Tay, "Rationalizing the coefficients of popular biorthogonal wavelet filters," *IEEE Trans. Circuits Syst. Video Technol.*, vol. 10, pp. 998–1005, Sep. 2000.

[30] M. Vetterli and J. Kovačević, *Wavelets and Subband Coding*. Englewood Cliffs, NJ: Prentice-Hall, 1995.

[31] H. Volkmer, "On the regularity of wavelets," *IEEE Trans. Inf. Theory*, vol. 38, pp. 872–876, Mar. 1992.

[32] D. X. Zhou, "Norms concerning subdivision sequences and their applications in wavelets," *Applied Comput. Harmonic Anal.*, vol. 11, pp. 329–346, 2001.

A. Farras Abdelnour (M'04) received the B.S., M.S., and Ph.D. in electrical engineering in 1988, 1990, and 2003, respectively, from Polytechnic University, Brooklyn, NY.

His thesis explores wavelet design using the Gröbner basis method. His current research interests include medical imaging, image denoising and enhancement, and filterbank and wavelet design. He is currently a Research Fellow with Memorial Sloan-Kettering Cancer Center, Medical Physics, New York, NY.

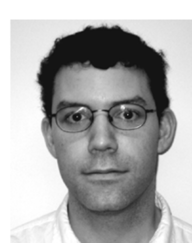

Ivan W. Selesnick (M'97) received the B.S., M.E.E., and Ph.D. degrees in electrical engineering in 1990, 1991, and 1996, respectively, from Rice University, Houston, TX.

In 1997, he was a visiting professor at the University of Erlangen-Nurnberg, Erlangen, Germany. Since 1997, he has been an assistant professor with the Department of Electrical and Computer Engineering, Polytechnic University, Brooklyn, NY. His current research interests are in the area of digital signal processing and wavelet-based signal processing.

Dr. Selesnick is currently a member of the IEEE Signal Processing Theory and Methods Technical Committee of the IEEE SP Society and an associate editor of the IEEE TRANSACTIONS ON IMAGE PROCESSING.